Biointerface Research in Applied Chemistry
Open-Access Journal (ISSN: 2069-5837)

Article
Volume 13, Issue 3, 2023, 228
https://doi.org/10.33263/BRIAC133.228

Developing a Sensing Platform based on Molecular Imprinting of HbA1c on Fe_3O_4 Nanoparticle Modified Screen-Printed Electrode

Sunil Kumar Mahobiya [1], Nidhi Chauhan [1], Sapna Balayan [1], Naresh Kumar Kuchhal [2], Saikh Safiul Islam [3], Utkarsh Jain [1,*]

[1] Amity Institute of Nanotechnology (AINT), Amity University Uttar Pradesh (AUUP), Sector -125, Noida- 201313, Uttar Pradesh, India; ksunil912@gmail.com (S.K.); nchauhan1@amity.edu (N.C.); sbalayan@amity.edu (S.B.); ujain@amity.edu (U.J.);
[2] Bio Diagnostic Laboratory, Rohini, Delhi-110085, India; nkkuchhal@gmail.com (N.K.K.);
[3] Centre For Nanoscience & Nanotechnology, Jamia Millia Islamia, Jamia Nagar, New Delhi-110025, India; sislam@jmi.ac.in (S.S.I.);
* Correspondence: ujain@amity.edu, karshjain@gmail.com (U.J.);

Scopus Author ID 56534847500

Received: 13.01.2022; Accepted: 29.03.2022; Published: 6.06.2022

Abstract: An individual's diabetic and pre-diabetic condition can be evaluated by measuring glycated hemoglobin (HbA1c) in the blood samples. This study aims to fabricate an electrochemical biosensor to identify HbA1c concentration in blood samples. The biosensor is developed based on molecularly imprinting technology and modified with iron oxide nanoparticles (Fe_3O_4). The nanoparticles enhanced the electrochemical activity on the electrode surface, while synthesized molecularly imprinted polymer (MIP) for HbA1c provided high specificity and selectivity on the fabricated interface. Each step was significantly characterized during the modification stages of the developed biosensor. As a result, the biosensor exhibits a wide detection range of 1 pM to 0.1 μM and a low detection limit of 1 pM. The fabricated biosensor requires very few drops of the blood sample and provides a fast response and long-term stability.

Keywords: Diabetes; Iron oxide; Molecularly imprinted polymer; Glycated hemoglobin; Electrochemical biosensor.

1. Introduction

Diabetes is observed as a chronic disease across the globe leading to premature death and several disabilities. The number of patients with diabetic conditions has increased in the last decades and is believed to rise further every year [1,2]. About 382 million cases were reported in 2013 and are expected to reach up to 592 million in 2035 [3,4]. Type 2 diabetes mellitus has been recorded as the general type of diabetes worldwide [5-7]. Type 2 diabetes is identified by hyperglycemia levels in the body leading to the change in fat, carbohydrate, and lipid metabolism and obstructed secretion of insulin in the pancreatic region. Glycated hemoglobin (HbA1c) has been reported as the standard gold method. This helps track the change in the glucose level in the blood for controlling glycemic conditions in individuals affected by diabetes mellitus. The assay developed for HbA1c monitoring provides accurate and precise results. Also, it facilitates the understanding of diabetes-associated complications and risks. Several international diabetes societies and World Health Organization (WHO) have

approved this test for clinical applications [8-10]. In 2010, based on the HbA1c level, a criterion was set for diabetic and pre-diabetic conditions by American Diabetic Association and International Expert Committee. If HbA1c lies between 5.7-6.4% (39-46 mM/M) then the condition is pre-diabetic whereas, if HbA1c ≥6.5% (≥48 mM/M) is considered as diabetic Mellitus [11-13].

The formation of HbA1c takes place with an irreversible glycation process that occurs regularly at a slow rate. It is a combination of sugar available in the serum and naive hemoglobin (Hb) in the red blood cells (RBC) [8]. Obesity is considered a major complication of irregular glucose levels in diabetes, and this has reached epidemic proportions. The hypothesis is that the individual with obesity has a higher risk of being diabetic when compared with a normal-weight person. A study has reported that a person suffering from obesity has a higher risk of the pre-diabetic condition.

Presently, various detection assays have been developed for the identification of HbA1c levels, for instance, high-performance liquid chromatography (HPLC) [8,12-15], immunoassay [16], thiobarbituric acid (TBA) assay, and boronate affinity. HPLC is the most preferred and commonly used technique, but it has some drawbacks such as high cost, requiring more quantity of solvents, trained expertise, large space for setting the instrument, and long analysis time. Therefore, developing an efficient method for the diagnosis of HbA1c is required. Recently, biosensors development is an emerging technology that is very much in demand for medical diagnosis [17-21].

This work aims to develop a biosensor based on evaluating electrochemical sensing changes to identify glycated hemoglobin concentration. A novel biosensing platform based on electrochemical measurement was designed and fabricated on the surface of a screen-printed electrode (SPE) integrated with nanomaterials and molecularly imprinted polymer. The biosensor was modified with iron oxide nanoparticles (Fe_3O_4NPs) to obtain higher activity on the electrode surface. The Fe_3O_4 nanoparticles facilitate improving the surface area on the electrode that enhances the transfer of electrons. Thus, the conductivity of the electrode is increased [22-24].

Further, the electrode surface was customized using synthesized molecularly imprinted polymer (MIP) for HbA1c. The MIP approach was used in developing the biosensor. These 3D matrices are highly specific to the biomolecules, providing high selectivity and sensitivity on the moderated electrode surface. The designed biosensing platform is highly selective and produces stable results; also, the sensor operates in a wide detection range. This designed biosensor on SPE can effectively be used for the potential application of HbA1c monitoring. The miniaturized size and rapid detection provide an advantage over the point-of-care devices.

2. Materials and Methods

*2.1. Chemicals and **a**pparatus.*

Methyl methacrylate (MMA), Ferrous chloride anhydrous ($FeCl_2$), Azobisisobutyronitrile (AIBN, 98%), Ethylene glycol dimethacrylate (EGDMA), Sodium hydroxide (NaOH), Ferric chloride anhydrous ($FeCl_3$), Glycated hemoglobin (HbA1c), Hydrochloric acid 37% (HCl), Acetonitrile (ACN) were procured from Sigma Aldrich. The screen-printed electrodes were acquired from PalmSens Compact Electrochemical Interfaces. All the solutions during experimentation were prepared in Distilled water (DW). Furthermore, modification of the fabricated surface of the SPE was examined using Scanning electron

microscopy (SEM) and electrochemical techniques with the help of a potentiostat (Biologics SPE-200) device.

2.2. Construction of Fe_3O_4NPs.

The co-precipitation method was adopted for synthesizing the Fe_3O_4NPs [22]. A mixture of $FeCl_3$ (0.03 M) and $FeCl_2$ (0.015 M) was prepared in a solution of 25 mL DW and 0.85 mL HCl (37%) with a continuous and vigorous stirring. A dropwise addition of $FeCl_3$ and $FeCl_2$ mixture in a 1.5 M NaOH (250 mL) was performed at room temperature and with continuous stirring. The mixture was kept for continuous stirring for 30 minutes to complete the nucleating process. Afterward, the obtained black precipitate was separated by centrifugation and washed with DW three times [23,24].

2.3. Synthesis of MIP.

Synthesis of MIP was carried out with a bulk polymerization process. The reagents, template-HbA1c, monomer-MMA, and crosslinker-EGDMA with specific ratios were dissolved in 50 mL of ACN solution and sonicated for 45 minutes. Afterward, nitrogen purging was carried out for 10 minutes. 200 mg of AIBN was added to initiate the reaction; while maintaining the inert condition, the prepared mixture was kept at 40 ℃ with continuous stirring for 2 days in a water bath to carry out the polymerization process. Finally, a white crystalline powder was obtained after 2 days. This procured powder was then washed to remove the molecules of HbA1c from its surface with a solution prepared using methanol-acetic acid 3 times. Then the product was dried at 60 ℃ and prepared into a powder by crushing it into fine particles [25-27].

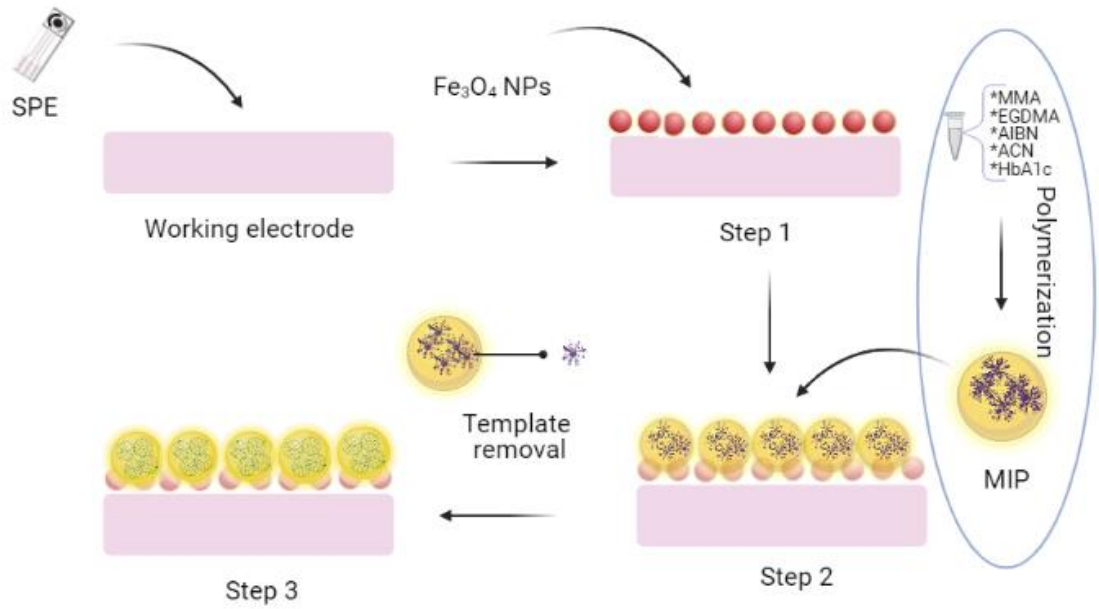

Scheme 1. Stepwise development of the biosensor for HbA1c: Step 1: Deposition of Fe_3O_4 nanoparticles on the surface of redesigned SPE; Step 2: Electrodeposition of molecularly imprinted polymer (MIP) on Fe_3O_4NPs/SPE; Step 3: Removal of a template (HbA1c) from MIP/Fe_3O_4NPs/SPE; SPE-Screen printed electrode; EGDMA-Ethylene glycol dimethylacrylate; AIBN-Azobisisobutyronitrile; HbA1c-Glycated Hemoglobin; MMA-Methyl methacrylate; MIP-Molecularly imprinted polymer; ACN-Acetonitrile.

2.4. Fabrication of working screen-printed electrode.

2.4.1 Electrochemically depositing Fe_3O_4 nanoparticles on SPE.

A mixture of 1 mg Fe_3O_4 nanoparticles in 1 mL of DW was prepared. This mixture was then used for electrodeposition of Fe_3O_4NPs. The electrodeposition of Fe_3O_4NPs was done using the chronoamperometry technique for 180 seconds in an electron mediator solution (5 mM- ferro-ferri) [28].

2.4.2. Modification of Fe_3O_4NPs/SPE with MIP.

The MIP synthesized for HbA1c was deposited on Fe_3O_4NPs coated SPE surface. For deposition of MIP on an electrode surface, the cyclic voltammetry (CV) technique was used at a scan rate of 20 mV/s when the potential was applied from -0.2 to +0.6 V (15 cycles) at a scan rate of 20 mV/s [25]. Afterward, the customized SPE was washed once to remove the unbounded reagents using DW, dried, and then used for experimentation. Scheme 1 describes the stepwise fabrication of the biosensor.

3. Results and Discussion

3.1. Surface study for developed MIP/Fe_3O_4NPs/SPE electrode.

The surface area, pore-volume, size, and diameter of synthesized molecularly imprinted polymer and the non-imprinted polymer (NIP) were obtained with Brunauer-Emmett-Teller (BET) analysis, as shown in Figures 1. (A) and (B), which depict the pore diameter and isotherm graph for synthesized MIP. The image describes that MIP is a microporous material [29,30]. The parameters obtained with BET analysis are summarized in Table 1. The pore diameter of the MIP was recorded as 3.772 nm, and the surface area was 5.316 m^2/g.

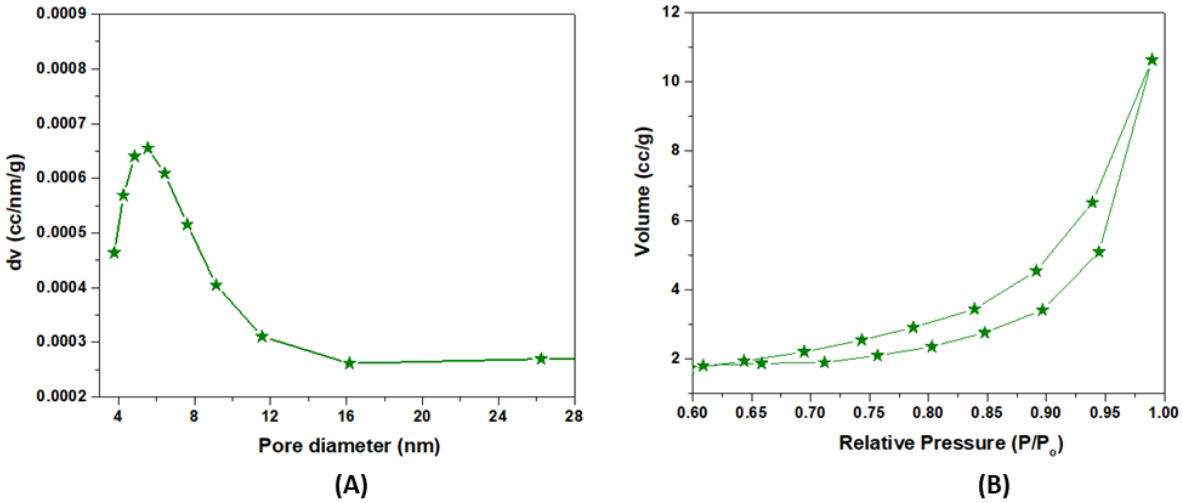

Figure 1. BET analysis for MIP: (A) Pore size distribution; (B) Adsorption and desorption.

Table 1. BET parameters for synthesized MIP.

Polymer	Surface area (m^2/g)	Volume of pore (cm^3/g)	Diameter of pore (nm)
Molecularly imprinted polymer (MIP)	5.316	0.017	3.772

The Fe_3O_4NPs were characterized with Energy-dispersive X-ray spectroscopy (EDX) as represented in Figure 2. The weight % of iron was obtained as 48.4%. Thereafter, the surface modification of fabricated SPE was studied with SEM (as illustrated in Figure 3). Figure 3(a)

shows the electrode surface coating with iron oxide nanoparticles. The spherical structures confirm the presence of nanoparticles. The Fe_3O_4NPs provide a large surface area and better catalytic property to the biosensor. Figure 3(b) describes the surface modification of the electrode with MIP for glycated hemoglobin molecules. The MIP provides high specificity and stability to the biosensor.

Further, the modified surface was washed using a mixture of methanol and acetic acid to remove the template. After that, the washing of the template resulted in the imprints of the HbA1c obtained, as shown in Figure 3(c). These imprints result in an enhanced diffusion rate of electron mediator on the electrode surface and higher electrical conductivity of the biosensor.

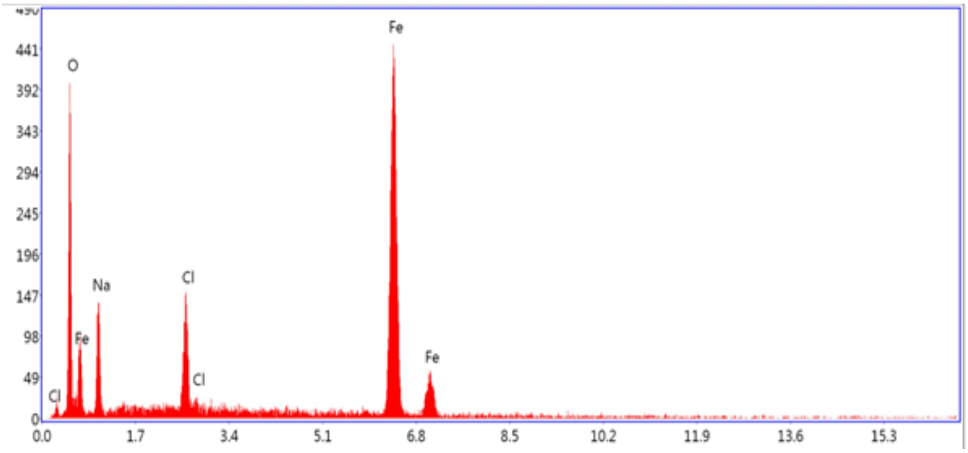

Figure 2. Energy-dispersive X-ray spectroscopy for Fe_3O_4 nanoparticles.

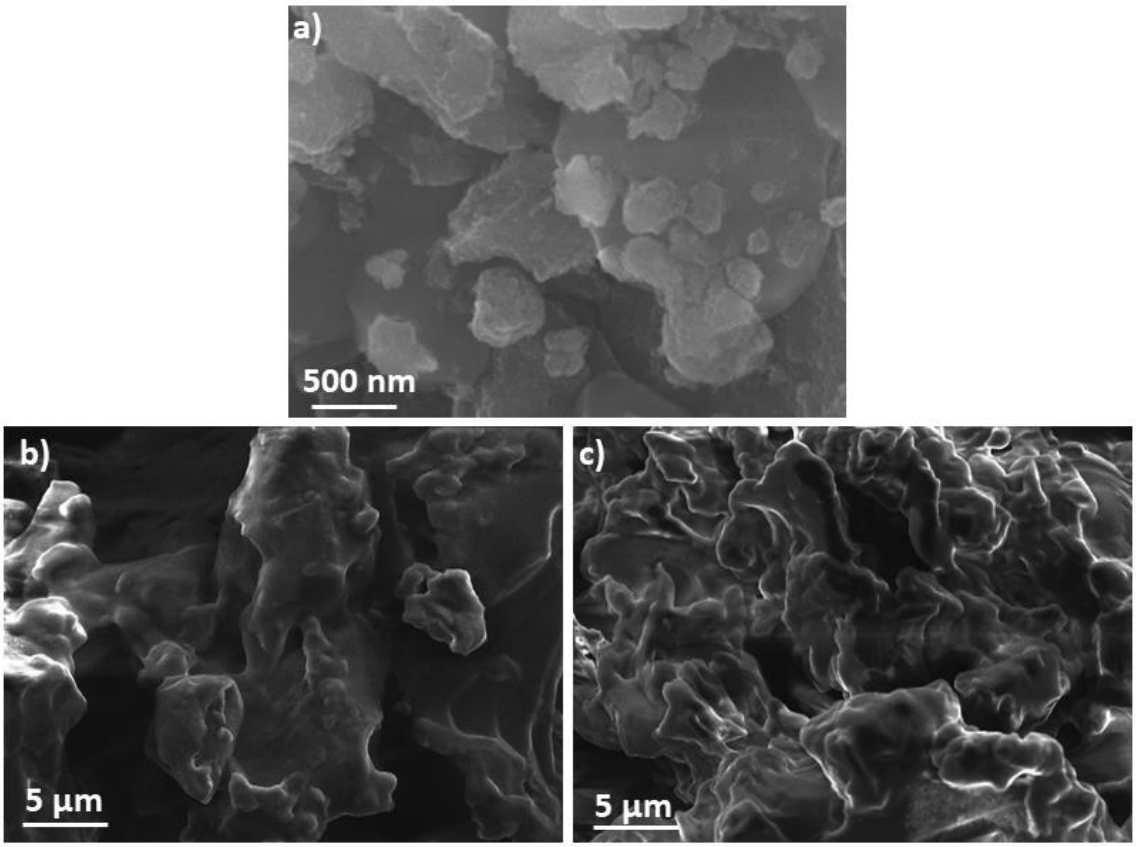

Figure 3. Scanning electron microscopy for stepwise modification of developed electrode (**a**) iron oxide nanoparticles; (**b**) Molecularly imprinted polymer with the template; (**c**) Molecularly imprinted polymer after template washing.

3.2. Electrochemical studies for modified stages of developed MIP/Fe_3O_4NPs/SPE electrode.

3.2.1. Cyclic voltammetry.

The modification stages of the designed SPE was examined using the CV technique. All these measurements were performed in ferro-ferri mediator solution (5 mM) under an applied potential from -1.0 to +1.0 V. Figure 4 describes the CV curve for each modification stage. The bare electrode shows the lowest anodic (Ipa) and cathodic (Ipc) peaks at +1.5 and -1.4 mA, respectively. The deposition of Fe_3O_4NPs on the surface of an SPE results in the enhancement of Ipa and Ipc to +2.6 and -2.4 mA due to the increased surface area, and the rate of electron charge transfer was significantly increased [31]. Afterward, when the surface of the SPE was modified with electrodeposition of MIP, the peaks were decreased due to the polymer. This restricts the current flow on an electrode surface. Whereas, after template removal, the anodic and cathodic peaks are again enhanced because eliminating the template from the MIP and the electrode generates more electroactive sites, increasing the charge transfer.

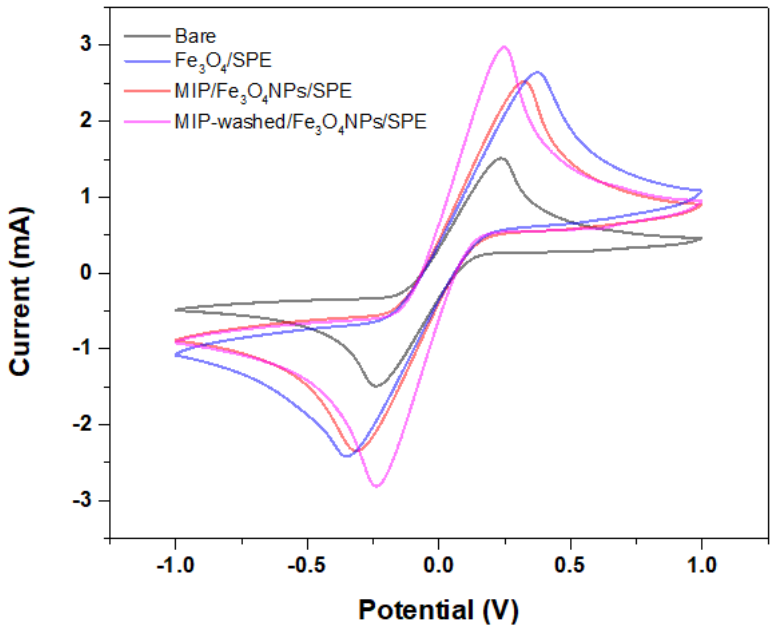

Figure 4. Cyclic voltammetry observation for every step: Bare SPE, Fe_3O_4NPs/SPE, MIP/ Fe_3O_4NPs/SPE, and MIP-washed/Fe_3O_4NPs/SPE performed in a electron mediator solution (5 mM- ferro-ferri) applying a potential from -1.0 to +1.0 V.

3.3. Optimization studies for MIP-washed/Fe_3O_4NPs/SPE biosensor.

3.3.1. Effect of concentration study on MIP-washed/Fe_3O_4NPs/SPE electrode.

The concentration effect was studied in a range from 1 pM to 0.1 μM. To study the concentration effect on an electrode surface, the electrochemical impedance spectroscopy (EIS) technique was incorporated. All the evaluations were performed in a 5 mM ferro-ferri solution and with frequency $F_{initial}$-100 KHz to F_{final}-100 mHz. Figure 5 illustrates the EIS graph for varying concentrations. It was evaluated that the Rct value is enhanced in the case of a higher concentration, whereas it decreases with the decreasing concentration. The higher Rct value was obtained at higher concentrations due to the blocking of molecule binding with the MIP; hence this causes an increase in resistance.

On the other hand, at lower concentrations, the molecules are free to bind with the MIP. Hence, low resistance is generated on the electrode surface [32-34]. The biosensor exhibits a low detection limit (1 pM).

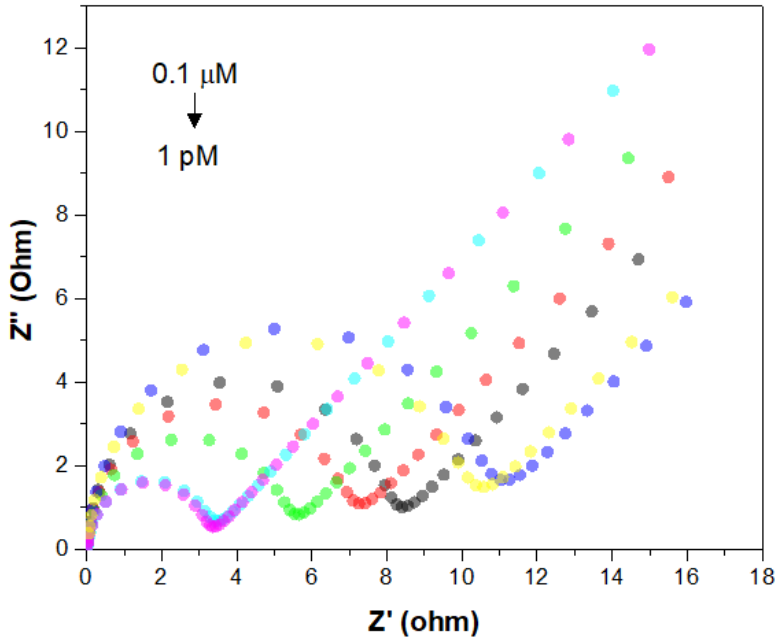

Figure 5. HbA1c concentration study with EIS technique ranging from 1 pM to 0.1 µM at frequency $F_{initial}$-100 KHz to F_{final}-100 mHz.

3.3.2. pH and temperature effect on the MIP-washed/Fe_3O_4NPs/SPE electrode.

The optimum pH of the designed biosensing platform was examined in a pH solution ranging from 5.5 to 8.5 pH. For the study of different pH values, the square wave voltammetry technique was adopted. Figure 6(A) describes the bar graph for different pH values and the peak current attained during the square wave voltammetry (SWV) measurements once performed in a ferrro-ferri solution (5 mM) while maintaining the steady potential (0.5 V). The graph explains that the electrode generates a higher current with the 7.5 pH solution. Beyond this pH, the current decreases because of the formation of hydrogen bonds on the surface of modified SPE [33]; therefore, the optimum pH was selected as 7.5 for all experiments.

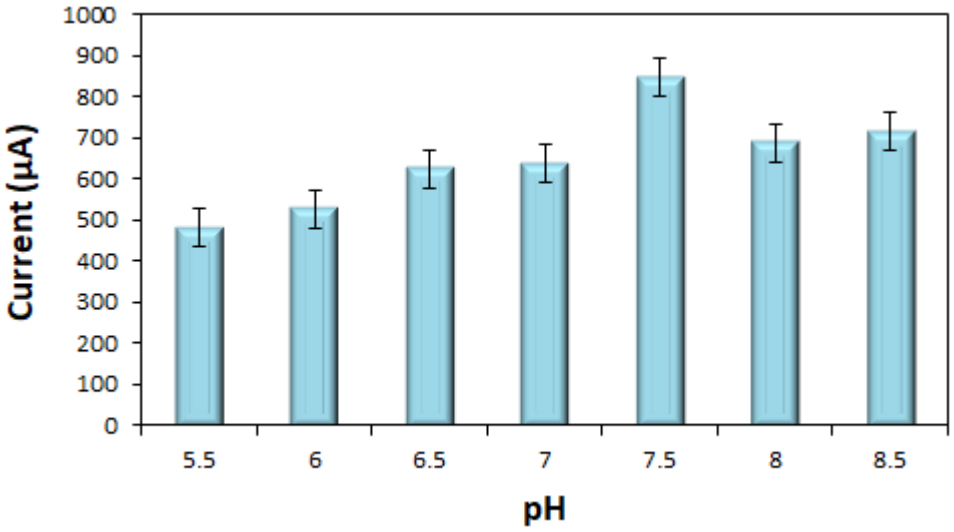

(A)

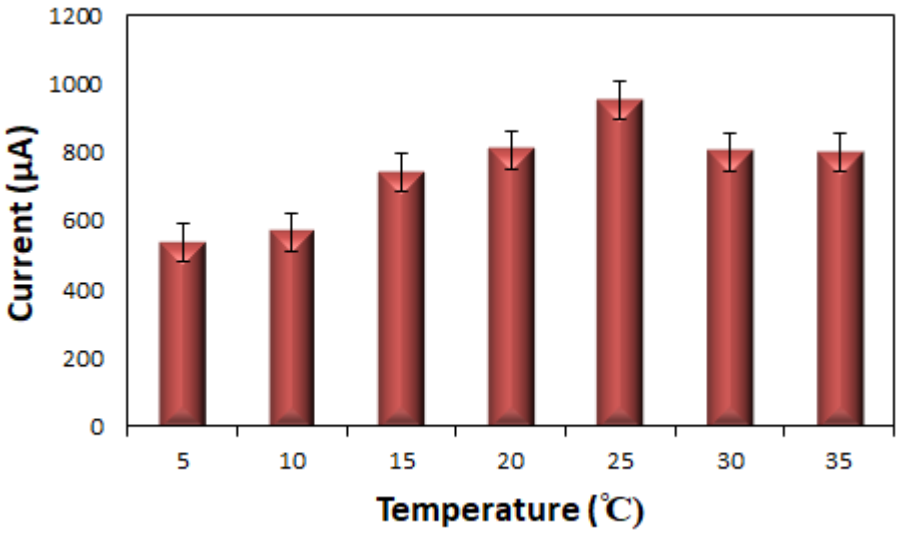

(B)

Figure 6. (**A**) Optimum pH study ranging from 5.5 to 8.5 with an interval of 0.5 units performed in ferro-ferri solution (5 mM) at -0.5 V; (**B**) Optimum temperature study for fabricated electrode ranging from 5℃ to 35℃ with each interval of 5 ℃.

The electrode was optimized with distinct temperature values from 5 to 35 °C after every 5°C interval. The current generated on the surface of the designed SPE was measured using the SWV technique with different temperatures in a ferro-ferri solution (5 mM). The applied potential was kept constant at -0.5 V for all the measurements. Figure 6(B) displays the peak current of SWV measurements for distinct temperature values. The highest current was obtained at 25 °C, and beyond this, the current value decreases; therefore, we considered 25 °C as the optimum temperature for the developed biosensor.

3.4. Validation of the developed biosensor.

3.4.1. Interference affecting the developed MIP-washed/Fe_3O_4NPs/SPE electrode.

The interference study was carried out on the electrode in a ferro-ferri solution (5 mM) with various compounds such as cholesterol ($C_{27}H_{46}O$) and glucose ($C_6H_{12}O_6$), acetylcholine (Ach), ascorbic acid ($C_6H_8O_6$), and uric acid ($C_5H_4N_4O_3$). Figure 7 illustrates the bar graph for different interference compounds and the activity of biosensors (%). The interfering compounds show less than 15% activity loss.

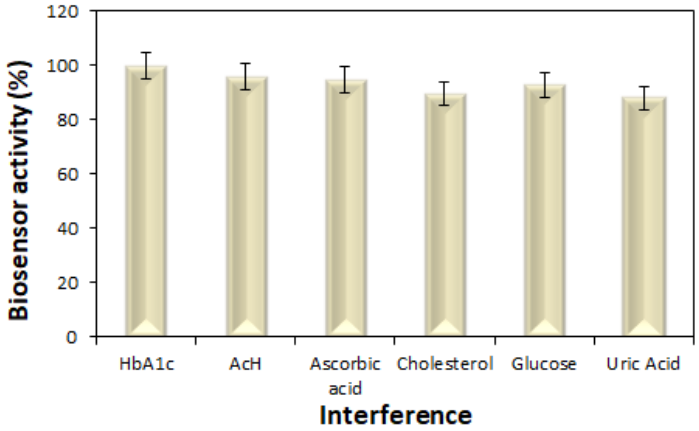

Figure 7. Effect of interference compounds on developed electrode performed in ferro-ferri mediator solution (5 mM) with concentration 1 pM.

3.4.2. Repeatability and stability of the designed electrochemical biosensing platform.

The repeatability of the fabricated SPE was investigated with five identical electrodes prepared simultaneously and following the same conditions. Figure 8 shows that the bar graph for these five electrodes displays a negligible current change. The current difference was observed in µA.

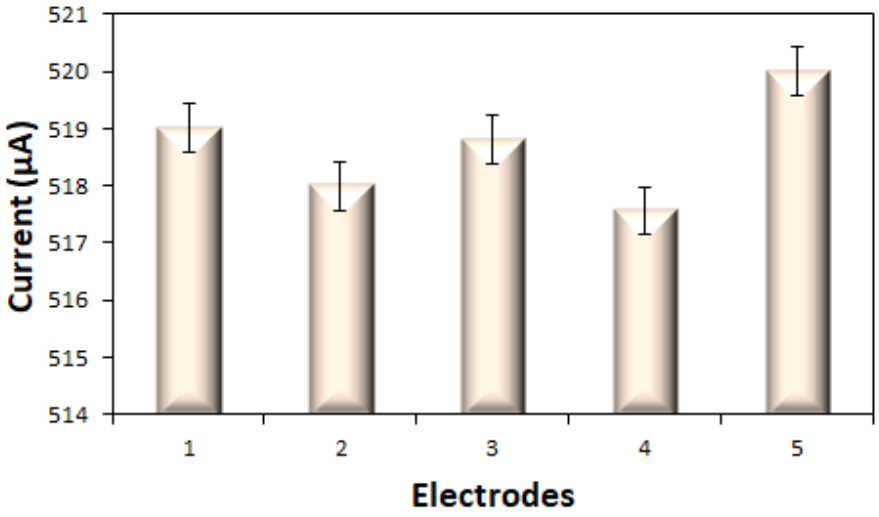

Figure 8. Reproducibility of the developed biosensor with similarly prepared electrodes under the same conditions.

To study the stability of the developed electrode, it was kept at 4 °C in a dry condition. The fabricated sensing platform was evaluated for 3 months. The activity of the designed SPE was examined every 7th day [35]. After 3 months, it was observed that the activity of the electrode decreased from 100% to 80%. Table 2 describes a comparison data for the reported and fabricated biosensors to detect HbA1c. The designed biosensing platform for HbA1c detection exhibits a dynamic concentration range and a very low detection limit.

Table 2. Comparison of the designed biosensor with reported for HbA1c detection

S.No.	Sensing platform	Biosensor type	Detection range	Detection limit	Reference
1.	SPCE/CNT-Nf@Blood-Nf	Electrochemical	31.2-500 nM	4.2 nM	[36]
2.	AuNPs/GNs/FTO	Electrochemical	10-65 µg/mL	1.70 µg/mL	[37]
3.	GS/rGO-Au nanostructure	Electrochemical	1 nM-13.83 µM	1 nM	[38]
4.	SPCE/pTBA@MWCNT	Electrochemical	0.006-0.74 µM	3.7 nM	[39]
5.	FPOX/AuNPs/GO/CHIT/FTO	Electrochemical	0.1-2 mM	0.3 µM	[40]
6.	4-MPBA-Au NFs modified SPCE	Electrochemical	5-1000 µg/mL	0.65%	[41]
7.	Aptasensor	Electrochemical	100 pg/mL-100 ng/mL	0.2 ng/mL	[42]
8.	MIP/Fe_3O_4NPs/SPE electrode	Electrochemical	1 pM-0.1 µM	1 pM	Present work

3.4.3. Clinical validation of the fabricated SPE-based biosensor.

To validate the electrode with clinical samples, the samples were spiked (sample A (1 nM), sample B (0.01 nM), sample C (0.1 pM), sample D (100 nM)), and the SWV technique was used to measure the electrode current. Figure 9 depicts the peak current values recorded during the SWV measurements. The highest current was observed with sample C, which had a low concentration of HbA1c. In contrast, the lowest current was observed with sample D representing a higher concentration of HbA1c in the sample.

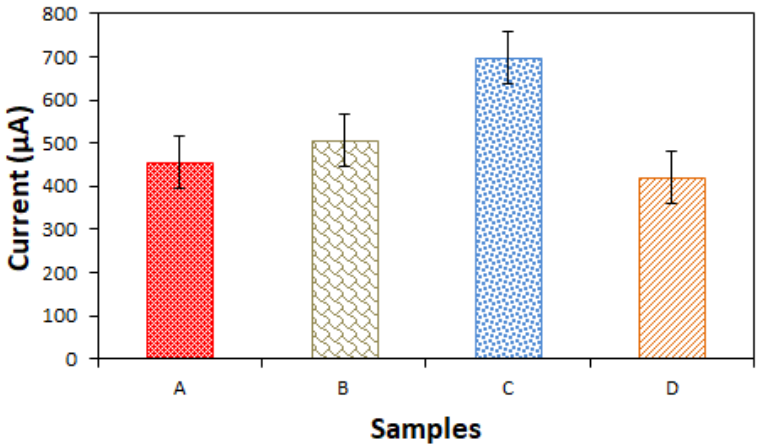

Figure 9. Graph for real blood samples on the modified versus current obtained.

4. Conclusions

An electrochemical biosensor was developed to detect HbA1c concentration in blood samples for diabetic conditions. The Fe_3O_4 nanoparticles were used to facilitate the higher conductivity of the developed biosensor by enhancing the electrode's surface area and thereby increasing the rate of transfer of electrons on the surface of the screen-printed electrode. The molecularly imprinted polymer enhances the selectivity and specificity of the developed biosensor by imprinting the molecule's predefined structure. The fabricated biosensor exhibits a dynamic concentration range from 1 pM to 0.1 µM and a low detection limit. The biosensor requires less sample quantity for detection, and therefore, it provides rapid results and satisfactory stability. The designed sensing platform can be advanced into a point of care (POC) device because of several advantages: miniaturized size, cost-effectiveness, rapid detection, and user-friendly approach.

Funding

This research received external funding from Biotechnology Industry Research Assistance Council (BIRAC) (File No. BT/IIPME0211/02/16).

Acknowledgments

The work was financially supported by Biotechnology Industry Research Assistance Council (BIRAC) (File No. BT/IIPME0211/02/16).

Conflicts of Interest

The authors declare no conflict of interest.

References

1. Pohanka, M. Glycated Hemoglobin and Methods for Its Point of Care Testing. *Biosensors* **2021**, *11*, 70, https://doi.org/10.3390/bios11030070.
2. American Diabetes Association. Introduction: standards of medical care in diabetes—2020. *Diabetes care* **2020**, *43*, S1-S2, https://doi.org/10.2337/dc20-Sint.
3. Faruque, L.I.; Wiebe, N.; Ehteshami-Afshar, A.; Liu, Y.; Dianati-Maleki, N.; Hemmelgarn, B.R.; Manns, B.J.; Tonelli, M. Effect of telemedicine on glycated hemoglobin in diabetes: a systematic review and meta-analysis of randomized trials. *Cmaj* **2017**, *189*, E341-E364, https://doi.org/10.1503/cmaj.150885.

4. Reed, J.; Bain, S.; Kanamarlapudi, V. A review of current trends with Type 2 diabetes epidemiology, aetiology, pathogenesis, treatments and future perspectives. *Diabetes, Metabolic Syndrome and Obesity: Targets and Therapy* **2021**, *14*, 3567, https://doi.org/10.2147/DMSO.S319895.
5. Izzo, A.; Massimino, E.; Riccardi, G.; Della Pepa, G. A Narrative Review on Sarcopenia in Type 2 Diabetes Mellitus: Prevalence and Associated Factors. *Nutrients* **2021**, *13*, 183, https://doi.org/10.3390/nu13010183.
6. Eslami, M.; Bahar, A.; Hemati, M.; Rasouli Nejad, Z.; Mehranfar, F.; Karami, S.; Kobyliak, N.M.; Yousefi, B. Dietary pattern, colonic microbiota and immunometabolism interaction: new frontiers for diabetes mellitus and related disorders. *Diabetic Medicine* **2021**, *38*, 14415, https://doi.org/10.1111/DME.14415.
7. Ng, A.C.; Delgado, V.; Borlaug, B.A.; Bax, J.J. Diabesity: the combined burden of obesity and diabetes on heart disease and the role of imaging. *Nature Reviews Cardiology* **2021**, *18*, 291-304, https://doi.org/10.1038/s41569-020-00465-5.
8. Zhang, H.; Li, D.; Yang, Y.; Chang, H.; Simone, G. On-resonance islands of Ag-nanowires sense the level of glycated hemoglobin for diabetes diagnosis. *Sensors and Actuators B: Chemical* **2020**, *321*, 128451, https://doi.org/10.1016/j.snb.2020.128451.
9. Liang, J.; Shi, X.; Feng, H.; Chen, M.; Li, W.; Lai, J.; Hu, W.; Li, G. 1, 5-anhydroglucitol biosensor based on light-addressable potentiometric sensor with RGO-CS-Fc/Au NPs nanohybrids. *Bioelectrochemistry* **2021**, *142*, 107938, https://doi.org/10.1016/j.bioelechem.2021.107938.
10. John, W.G.; Hillson, R.; Alberti, S.G.; Use of haemoglobin A1c (HbA1c) in the diagnosis of diabetes mellitus. The implementation of World Health Organisation (WHO) guidance 2011. *Practical Diabetes* **2012**, *29*, 12-12a, https://doi.org/10.1002/pdi.1648.
11. Shorey, S.; Ng, E.D.; Law, E.C.; Wong, J.C.; Loke, K.Y.; San Tam, W.W. Physical activity interventions and nutrition-based interventions for children and adolescents with type 1 diabetes mellitus. *Cochrane Database of Systematic Reviews* **2021**, *1*, https://doi.org/10.1002/14651858.CD013858.
12. Altuntaş, S.Ç.; Evran, M.; Gürkan, E.; Sert, M.; Tetiker, T. HbA1c level decreases in iron deficiency anemia. *Wiener klinische Wochenschrift* **2021**, *133*, 102-106, https://doi.org/10.1007/s00508-020-01661-6.
13. Pasquel, F.J.; Lansang, M.C.; Dhatariya, K.; Umpierrez, G.E. Management of diabetes and hyperglycaemia in the hospital. *The Lancet Diabetes & Endocrinology* **2021**, *9*, 174-188, https://doi.org/10.1016/S2213-8587(20)30381-8.
14. Gonzalez-Viveros, N.; Castro-Ramos, J.; Gomez-Gil, P.; Cerecedo-Nunez, H.H. Characterization of glycated hemoglobin based on raman spectroscopy and artificial neural networks. *Spectrochimica Acta Part A: Molecular and Biomolecular Spectroscopy* **2021**, *247*, 119077, https://doi.org/10.1016/j.saa.2020.119077.
15. Gupta, S.; Jain, U.; Chauhan, N. Laboratory diagnosis of HbA1c: a review. *J Nanomed Res* **2017**, *5*, 00120, https://doi.org/10.15406/jnmr.2017.05.00120.
16. Wu, C.C.; Lin, H.I.; Chang, K.W.; Mai, J.D.; Shiesh, S.C.; Lee, G.B.Measurement of glycated hemoglobin levels using an integrated microfluidic system. *Microfluidics and Nanofluidics* **2015**, *18*, 613-621, https://doi.org/10.1007/s10404-014-1460-5.
17. Jain, U.; Gupta, S.; Chauhan, N. Detection of glycated hemoglobin with voltammetric sensing amplified by 3D-structured nanocomposites. *International journal of biological macromolecules* **2017**, *101*, 896-903, https://doi.org/10.1016/j.ijbiomac.2017.03.127.
18. Jain, U.; Chauhan, N. Glycated hemoglobin detection with electrochemical sensing amplified by gold nanoparticles embedded N-doped graphene nanosheet. *Biosensors and Bioelectronics* **2017**, *89*, 578-584, https://doi.org/10.1016/j.bios.2016.02.033.
19. Jain, U.; Singh, A.; Kuchhal, N.K.; Chauhan, N. Glycated hemoglobin biosensing integration formed on Au nanoparticle-dotted tubular TiO_2 nanoarray. *Analytica chimica acta* **2016**, *945*, 67-74, https://doi.org/10.1016/j.aca.2016.09.026.
20. Chauhan, N.; Jain, U. Influence of Zinc Oxide Nanorods on the Sensitivity of A Glycated Hemoglobin Biosensor. *Adv. Mater. Lett* **2016**, *7*, 666-672, https://doi.org/10.5185/amlett.2016.6177.
21. Jain, U.; Gupta, S.; Chauhan, N. Construction of an amperometric glycated hemoglobin biosensor based on Au–Pt bimetallic nanoparticles and poly (indole-5-carboxylic acid) modified Au electrode. *International journal of biological macromolecules* **2017**, *105*, 549-555, https://doi.org/10.1016/j.ijbiomac.2017.07.084.
22. Xiang, H.; Ren, G.; Zhong, Y.; Xu, D.; Zhang, Z.; Wang, X.; Yang, X. Fe_3O_4@C Nanoparticles Synthesized by In Situ Solid-Phase Method for Removal of Methylene Blue. *Nanomaterials* **2021**, *11*, 330, https://doi.org/10.3390/nano11020330.

23. Chauhan, N.; Narang, J.; Jain, U. Amperometric acetylcholinesterase biosensor for pesticides monitoring utilising iron oxide nanoparticles and poly (indole-5-carboxylic acid). *Journal of Experimental Nanoscience*, **2016**, *11*, 111-122, https://doi.org/10.1080/17458080.2015.1030712.
24. Sanaeifar, N.; Rabiee, M.; Abdolrahim, M.; Tahriri, M.; Vashaee, D.; Tayebi, L. A novel electrochemical biosensor based on Fe_3O_4 nanoparticles-polyvinyl alcohol composite for sensitive detection of glucose. *Analytical Biochemistry* **2017**, *519*, 19-26, https://doi.org/10.1016/j.ab.2016.12.006.
25. Jain, U.; Soni, S.; Balhara, Y.P.S.; Khanuja, M.; Chauhan, N. Dual-Layered Nanomaterial-Based Molecular Pattering on Polymer Surface Biomimetic Impedimetric Sensing of a Bliss Molecule, Anandamide Neurotransmitter. *ACS omega* **2020**, *5*, 10750-10758, https://doi.org/10.1021/acsomega.0c00285.
26. Balayan, S.; Chauhan, N.; Chandra, R.; Jain, U. Molecular imprinting based electrochemical biosensor for identification of serum amyloid a (SAA), a neonatal sepsis biomarker. *International Journal of Biological Macromolecules* **2021**, *195*, 589-597, https://doi.org/10.1016/j.ijbiomac.2021.12.045.
27. Balayan, S.; Chauhan, N.; Kumar, P.; Chandra, R.; Jain, U. Fabrication of a sensing platform for identification of tumor necrosis factor-alpha: a biomarker for neonatal sepsis. *3 Biotech* **2022**, *12*, 1-13, https://doi.org/10.1007/s13205-021-03083-1.
28. Qian, X.; Xu, Q.; Hang, T.; Shanmugam, S.; Li, M. Electrochemical deposition of Fe_3O_4 nanoparticles and flower-like hierarchical porous nanoflakes on 3D Cu-cone arrays for rechargeable lithium battery anodes. *Materials & Design* **2017**, *121*, 321-334, https://doi.org/10.1016/j.matdes.2017.02.080.
29. Qi, L.; Tang, X.; Wang, Z.; Peng, X. Pore characterization of different types of coal from coal and gas outburst disaster sites using low temperature nitrogen adsorption approach. *International Journal of Mining Science and Technology* **2017**, *27*, 371-377, https://doi.org/10.1016/j.ijmst.2017.01.005.
30. Adu, A.A.; Neolaka, Y.A.; Riwu, A.A.P.; Iqbal, M.; Darmokoesoemo, H.; Kusuma, H.S. Synthesis, characterization and evaluation of swelling ratio on magnetic p53-poly (MAA-co-EGDMA)@ GO-Fe_3O_4 (MIP@ GO-Fe_3O_4)-based p53 protein and graphene oxide from kusambi wood (Schleichera oleosa). *Journal of Materials Research and Technology* **2020**, *9*, 11060-11068, https://doi.org/10.1016/j.jmrt.2020.08.003.
31. Chauhan, N.; Pundir, C.S. An amperometric acetylcholinesterase sensor based on Fe_3O_4 nanoparticle/multi-walled carbon nanotube-modified ITO-coated glass plate for the detection of pesticides. *Electrochimica Acta* **2012**, *67*, 79-86, https://doi.org/10.1016/j.electacta.2012.02.012.
32. Nguy, T.P.; Van Phi, T.; Tram, D.T.; Eersels, K.; Wagner, P.; Lien, T.T. Development of an impedimetric sensor for the label-free detection of the amino acid sarcosine with molecularly imprinted polymer receptors. *Sensors and Actuators B: Chemical* **2017**, *246*, 461-470, https://doi.org/10.1016/j.snb.2017.02.101.
33. Aydın, E.B.; Aydın, M.; Sezgintürk, M.K. Immunosensors Based on the Technology of Molecular Imprinted Polymers. In *Molecular Imprinting for Nanosensors and Other Sensing Applications* **2021**, 117-161, https://doi.org/10.1016/B978-0-12-822117-4.00006-X.
34. Yusof, N.A.; Rahman, S.K.A.; Hussein, M.Z.; Ibrahim, N.A. Preparation and characterization of molecularly imprinted polymer as SPE sorbent for melamine isolation. *Polymers* **2013**, *5*, 1215-1228, https://doi.org/10.3390/polym5041215.
35. Singh, A.P.; Balayan, S.; Gupta, S.; Jain, U.; Sarin, R.K.; Chauhan, N. Detection of pesticide residues utilizing enzyme-electrode interface via nano-patterning of TiO_2 nanoparticle and molybdenum disulfide (MoS_2) nanosheets. Process Biochemistry **2021**, *108*, 185-193, https://doi.org/10.1016/j.procbio.2021.06.015.
36. Thiruppathi, M.; Lee, J.F.; Chen, C.C.; Ho, J.A.A. A disposable electrochemical sensor designed to estimate glycated hemoglobin (HbA1c) level in whole blood. *Sensors and Actuators B: Chemical* **2021**, *329*, 129119, https://doi.org/10.1016/j.snb.2020.129119.
37. Li, M.; Zhao, W.J.; Tian, L.L.; Li, H.F.; Fan, B. Fabrication of biosensor for selective electrochemical determination of glycated hemoglobin. *Int. J. Electrochem. Sci* **2017**, *12*, 8411-8420, https://doi.org/10.20964/2017.09.09.
38. Jaberi, S.Y.S.; Ghaffarinejad, A.; Omidinia, E. An electrochemical paper based nano-genosensor modified with reduced graphene oxide-gold nanostructure for determination of glycated hemoglobin in blood. *Analytica chimica acta* **2019**, *1078*, 42-52, https://doi.org/10.1016/j.aca.2019.06.018.
39. Moon, J.M.; Kim, D.M.; Kim, M.H.; Han, J.Y.; Jung, D.K.; Shim, Y.B. A disposable amperometric dual-sensor for the detection of hemoglobin and glycated hemoglobin in a finger prick blood sample. *Biosensors and Bioelectronics* **2017**, *91*, 128-135, https://doi.org/10.1016/j.bios.2016.12.038.
40. Shahbazmohammadi, H.; Sardari, S.; Omidinia, E. An amperometric biosensor for specific detection of glycated hemoglobin based on recombinant engineered fructosyl peptide oxidase. *International journal of biological macromolecules* **2020**, *142*, 855-865, https://doi.org/10.1016/j.ijbiomac.2019.10.025.

41. Wang, X.; Su, J.; Zeng, D.; Liu, G.; Liu, L.; Xu, Y.; Wang, C.; Liu, X.; Wang, L.; Mi, X. Gold nano-flowers (Au NFs) modified screen-printed carbon electrode electrochemical biosensor for label-free and aquantitative detection of glycated hemoglobin. *Talanta* **2019**, *201*, 119-125, https://doi.org/10.1016/j.talanta.2019.03.100.
42. Eissa, S.; Zourob, M. Aptamer-based label-free electrochemical biosensor array for the detection of total and glycated hemoglobin in human whole blood. *Scientific reports* **2017**, *7*, 1-8, https://doi.org/10.1038/s41598-017-01226-0.